SYNTHESES AND REFLECTANCE ANALYSES OF LUNAR RED GLASS COMPOSITIONS: INFORMATION TO IMPROVE UNDERSTANDING OF REMOTELY SENSED SPECTRAL DATA.

J. J Gillis-Davis[1], P. G. Lucey[1], J. E. Hammer[2], and B. B. Wilcox[1], University of Hawaii at Manoa, Hawaii Institute for Geophysics and Planetology[1], and Geology & Geophysics[2], 1680 East-West Road, POST 503, Honolulu, HI 96744, USA (gillis@higp.hawaii.edu).

Introduction: Compositions of many of the >100 lunar pyroclastic deposits identified remotely are poorly constrained. In addition, the absorption properties of glasses, which are ubiquitous in all regolith samples, strongly influence spectra of lunar soil and hence spectral remote sensing data of the lunar surface [1,2]. Previous spectral studies of lunar synthetic glasses have not reproduced all lunar glass compositions (Fig 1). To this end, synthetic glasses are made with specific compositions (Table 1) and under controlled oxygen fugacity to facilitate study of the relationship between the optical properties of "lunar" glass and FeO, TiO_2 concentrations. Although the UV absorption is controlled by the sum of Fe and Ti, their relative importance is unknown. Also, the effect of Fe and Ti is believed restricted to the UV on the basis of little evidence. Thus, optical constants derived from this work have direct application to radiative transfer modeling of lunar pyroclastic glasses [3] and agglutinates by providing the ability to evaluate the relative effects of Fe and Ti and determine whether Fe-Ti has any affect outside the UV. The goal is to eventually use our derived optical constants to match the remotely sensed spectral data with model data, and from this infer the composition of the lunar surface.

Methods: *Sample Synthesis*. The synthetic red glass composition for this study was based on the average lunar red glass composition (Table 1), and was synthesized with reagent-grade carbonate and oxide powders. The powders are heated for 30 minutes at 850°C in a controlled fO_2 environment. Flowing H_2-CO_2 gas mixture was used to impart an intrinsic fO_2 just above iron-wüstite to simulate lunar conditions. The sample is then lowered further into the furnace, where it is quickly (~1 min) heated above the liquidus temperature (~1400 °C), and then rapidly quenched. Quench is achieved when the crucible is tipped, allowing the molten sample to fall into a reservoir of water below the furnace.

Spectral analysis requires a relatively large quantity of homogenized glass. This obviates the use of the conventional Pt wire loop method. High purity alumina crucibles allow gram-quantities of material to be conditioned and fused at once. Additional advantages of this ceramic are its low cost, stability at low fO_2, and highly refractory nature. The compositional contrast between our lunar basalt compositions, which are strongly undersaturated in alumina, and the alumina container materials pose a potential contamination problem. Our preliminary experiments, however, exhibited minimal reaction with the container (Table 1), and the melt formed a ball inside the container (i.e., did not wet the container).

Table 1. Compositions of average lunar red glass, reagent reproduction, and average and standard deviation of 2 microprobe analyses of the glass.

	Average Red Glass	Reagent Composition	Microprobe Analyses	Standard Deviation
SiO2	35.04	35.09	33.32	0.67
TiO2	14.9	14.9	16.44	0.54
Al2O3	5.78	5.79	7.78	0.43
FeO	22.42	22.43	21.02	0.39
MgO	12.81	12.83	11.12	0.29
CaO	7.24	7.25	7.73	0.02
Na2O	0.36	0.37	0.30	0.01
K2O	0.14	0.15	0.12	0.01
Cr2O3	0.89	0.89	0.31	0.05
Sum	99.58	99.7	98.1	

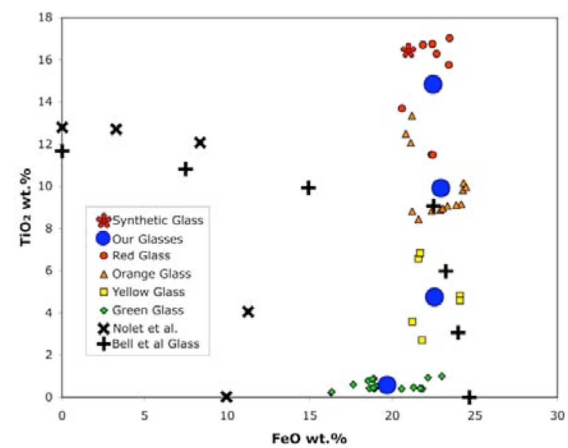

Fig 1. FeO and TiO_2 compositions for our proposed and synthesized glasses, previously made synthetic glasses [7,8], and lunar glass compositions from [9].

Measuring Reflectance and Deriving Optical Constants. Bidirectional reflectance measurements of synthetic lunar glass allow the calculation of optical constants of glasses using radiative transfer theory. The synthetic red glass samples have sufficient optical defects at the macroscopic level (Fig 2) to prohibit standard transmission methods for deriving absorption coefficients. Instead, our samples were ground and dry sieved to achieve a fine <53 μm powder. Reflectance measurements were made at the University of Hawaii using an Analytical Spectral Devices© spectrometer, which has a spectral range from 0.35 to 2.5 μm and a spectral resolution of 1 μm. Reflectance measurements are compared against a Spectralon reflectance standard. A quartz-halogen lamp was used as the illumination source, with a 40° incidence angle and 0° emission angle. Additional reflectance measurements will be made at Brown University's Reflectance Laboratory for comparison and reproducibility.

Optical constants were computed from the reflectance values of these powers using the methods of [4,5], as implemented by [6] for deriving mineral optical constants. While other methods are available to derive these constants, these methods require optically high-quality samples. As previously stated, our synthetic samples have macroscopic optical defects that invalidate transmission methods for deriving absorption coefficients.

Results: The glass produced is homogenous with only minor inclusions (Fig. 2). The composition of our glass closely matches the composition of the average lunar red glass (Table 1). The synthetic and authentic red glasses differ with respect to alumina content, but this difference is not expected to greatly affect the reflectance spectrum, as Al_2O_3 does not produce an absorption band or factor into the crystal field effect.

Fig. 3 shows reflectance spectra from 0.4 to 2.0 μm of the synthetic glass. Two bands are resolved near 1.0 and 1.9 μm, corresponding to crystal-field transitions in octahedrally and tetrahedrally coordinated Fe^{2+} ions, respectively [7]. The similarity between spectra of iron-bearing glass and pyroxene is due to the fact that much of the Fe^{2+} in glass is located in distorted octahedral sites similar to the M2 site in pyroxene. The absorption bands are broader and shallower than pyroxene because of short-range crystal order in glass. A strong slope is also evident in the 0.4-0.7 μm range. The slope is a charge-transfer band caused by the Fe^{2+}–Ti^{4+} coupled interaction [7]. The steepness of 400-700 nm slope is a direct proportion of the Fe^{2+}–Ti^{4+} concentration. The reflectance data of the synthetic red glass are compared to calculated reflectance of glass of similar composition and grain size, and without space weathering [3], and a sieved Apollo 11 soil sample (Fig. 3). All three spectra show similar absolute reflectance values. The Apollo 11 soil is expectedly bluer than either red glass. The spectrum of the synthetic glass is much less red and exhibits greater absorption around 2 μm than the radiative transfer calculated reflectance data.

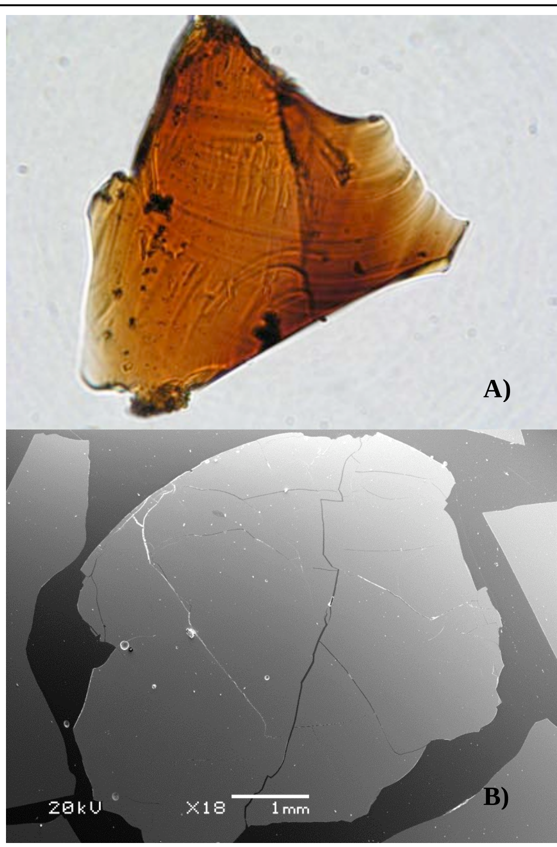

Fig 2. Both images show the compositional homogeneity of our synthesized "lunar" red glass A) Photomicrograph, the field of view is 0.6 mm. B) SEM backscatter image with 1mm scale bar.

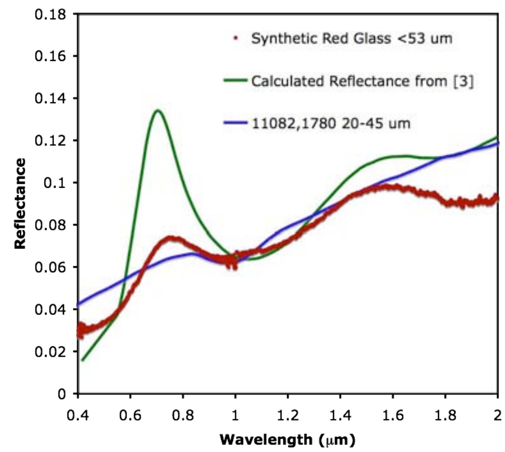

Fig 3. Reflectance of synthetic red glass particles and for comparison Apollo 11 soil sample 11084 from [10].

Conclusions: We synthesized a large volume of highly refractory lunar red glass compositions under lunar-like oxygen fugacities that are compositionally homogeneous and nearly crystal/inclusion free. Spectral features at 0.4 and 1.0 μm are caused by Fe^{2+} and Ti^{4+}, which give rise to the red color of the glass. The spectral difference between the synthetic glass and calculated spectra suggests that either differences in crystal field effects caused by multiple cations contained in the synthetic sample are not accounted for in the radiative transfer model data, or that uncertainties in optical coefficients derived from the Bell et al. [7] data are significant. Future optical constants derived from each of the four major lunar glass compositions (e.g., Fig. 1) will allow us better resolve these possibilities.

References: [1] Pieters C. M. (1993) Topics in remote sensing 4, pp. 594. [2] Hapke B. (2001) *JGR, 106 (E5)*, 10,039-10,073 [3] Wilcox B. B. et al. (2006) *JGR, 111*, doi:10.1029/2006JE002686. [4] Hapke B. (1981) *JGR, 86(B4)*, 3039-3054. [5] Hapke B. (1993) Theory of reflectance and emittance spectroscopy. Cambridge Univ. Press, Cambridge. [6] Lucey P. G. (1998) JGR, 103, 1703-1714. [7] Bell P. M. et al (1976) *Proc. Lunar Sci. Conf. 7th*, 2543-2559. [8] Nolet D. A. et al (1979) *Proc. Lunar Sci. Conf. 10th*, 1775-1786. [9] Delano J (1986) *Proc. Lunar Sci. Conf. 10th*, D201-D213. [10] Fischer E. M. & Pieters C. M. (1996) *JGR, 100(E11)*, 2225-2234.